Polyhedron 132 (2017) 70–77

Contents lists available at ScienceDirect

Polyhedron

journal homepage: www.elsevier.com/locate/poly

Palladium(II)/*N*,*N*-disubstituted-*N*′-acylthioureas complexes as anti-*Mycobacterium tuberculosis* and anti-*Trypanosoma cruzi* agents

Ana M. Plutín [a,*], Anislay Alvarez [a], Raúl Mocelo [a], Raúl Ramos [a], Eduardo E. Castellano [b], Monize M. da Silva [c], Wilmer Villarreal [c], Fernando R. Pavan [d], Cássio Santana Meira [e], José Simão Rodrigues Filho [e], Diogo Rodrigo M. Moreira [e], Milena Botelho P. Soares [e,f], Alzir A. Batista [c,*]

[a] Laboratorio de Síntesis Orgánica, Facultad de Química, Universidad de La Habana, La Habana, Cuba
[b] Instituto de Física de São Carlos, Universidade de São Paulo, São Carlos, SP, Brazil
[c] Departamento de Química, Universidade Federal de São Carlos, CEP 13.565-905 São Carlos, SP, Brazil
[d] Faculdade de Ciências Farmacêuticas, UNESP, Araraquara, SP, Brazil
[e] Instituto Gonçalo Moniz, Fundação Oswaldo Cruz, CEP 40296-750 Salvador, BA, Brazil
[f] Centro de Biotecnologia e Terapia Celular, Hospital São Rafael, CEP 41253-190 Salvador, BA, Brazil

ARTICLE INFO

Article history:
Received 30 January 2017
Accepted 1 May 2017
Available online 10 May 2017

Keywords:
Metal complexes
Palladium
Thioureas
Tuberculosis
Trypanosoma cruzi

ABSTRACT

The new complexes of Pd(II) with *N*,*N*-disubstituted-*N*′-acylthioureas:[(**1**) [Pd(dppf)(*N*,*N*-dimethyl-*N*′-benzoylthioureato-k^{2}O,S)]PF_6, (**2**) [Pd(dppf)(*N*,*N*-diethyl-*N*′-benzoylthioureato-k^{2}O,S)]PF_6, (**3**) [Pd(dppf)(*N*,*N*-dibuthyl-*N*′-benzoylthioureato-k^{2}O,S)]PF_6, (**4**) [Pd(dppf)(*N*,*N*-diphenyl-*N*′-benzoylthioureato-k^{2}O,S)]PF_6, (**5**) [Pd(dppf)(*N*,*N*-diethyl-*N*′-furoylthioureato-k^{2}O,S)]PF_6, (**6**) [Pd(dppf)(*N*,*N*-diphenyl-*N*′-furoylthioureato-k^{2}O,S)]PF_6, (**7**) [Pd(dppf)(*N*,*N*-dimethyl-N′- thiophenylthioureato-k^{2}O,S)]PF_6, and (**8**) [Pd(dppf)(*N*,*N*-diphenyl-N′-thiophenylthioureato-k^{2}O,S)]PF_6, were prepared and characterized by elemental analysis, and spectroscopic techniques. The structures of complexes (**2**), (**3**), (**5**), (**6**) and (**8**) had their structures determined by X-ray crystallography, confirming the coordination of the ligands with the metal through sulfur and oxygen atoms, forming distorted square-planar geometries. These complexes have shown antibacterial activity against anti-*Mycobacterium tuberculosis* H37Rv ATCC 27294. The complexes exhibited antiparasitic activity against *Trypanosoma cruzi*, while the metal-free thioureas did not. The results demonstrated that the compounds described here can be considered as promising anti-*Mycobacterium tuberculosis* and anti-*T. cruzi* agents, since in both cases their *in vitro* activity were better than reference drugs available for the treatment of both diseases.

1. Introduction

The *Mycobacterium tuberculosis* (MTB), causative agent of tuberculosis, is responsible for the death of around 2–3 million people, annually, and a global economic toll of U$12 billion each year [1]. The rise of multidrug resistance (MDR) in MTB has complicated and prolonged the treatment. Therefore, no new drugs have been developed specifically against mycobacteria since the 1960s [2]. Thus, there is a great need to develop new therapeutic agents to treat tuberculosis, so as to reduce the total duration of treatment and to provide more effective drugs against MDR TB and latent tuberculosis infection. This involves the development of new therapeutic strategies against bacterial infection, which becomes more stringent, and one reason for this is mainly due the bacterial drug resistance to currently administered treatments.

Also, Chagas disease, caused by the protozoan parasite *Trypanosoma cruzi* (*T. cruzi*), affects approximately 10 million people worldwide, with a high prevalence in Latin America [3]. The few drugs available, benznidazole and nifurtimox, are only effective in curing when administered during the acute phase, but not effective in patients that have progressed to the chronic phase [4]. Furthermore, these drugs are not considered ideal, due to their severe side effects [5]. Thus, the search for new anti-*T. cruzi* compounds is also needed.

One strategy for the development of antimycobacterial and antiparasitic agents from the inorganic point of view is to use an organic compound, which already exhibit antibacterial property, as ligand, to form metal complexes. Thus, good candidates for this purpose are thiourea and their derivatives, which are known for their antiviral, antibacterial and cytotoxic properties [6]. There

* Corresponding author. Fax: +55 16 3351 8350.
E-mail address: daab@ufscar.br (A.A. Batista).

http://dx.doi.org/10.1016/j.poly.2017.05.003
0277-5387/

are several works in the literature demonstrating the activity of this class of compounds, against parasites such as *Plasmodium falciparum*, *Trypanosoma brucei* and *T. cruzi* [7]. In recent years, a number of urea, thiourea and acylthiourea derivatives containing (*R*)-2-amino-1-butanol were evaluated against *Mycobacterium tuberculosis* strains H37Rv ATCC 27294, showing good anti-tuberculosis effect, and the complexing capacity of thiourea derivatives have been reported [8–9].

The biological activity of complexes containing thiourea derivatives has been successfully screened for various biological processes and they exhibit a wide range of biological activities, including antifungal, anticancer [9–10] and insecticidal activities [11]. Therefore, in order to extend the research on potential metallodrugs aiming the *M. Tuberculosis* and Chagas disease we report here on some palladium complexes containing the bis (diphenylphosphine)ferrocene and *N*,*N*-disubstituted-*N*′-acyl thioureas as ligands. Detailed descriptions of synthesis and characterization of the ligands have been reported elsewhere [12]. The Pd (II)/*N*,*N*-disubstituted-*N*′-acyl thioureas complexes described in this work were synthesized, structurally characterized and were tested for their anti-*M. tuberculosis* and anti-*T. cruzi* activity, showing good results.

2. Experimental

2.1. Materials and measurements

The dichloro[bis(diphenylphosphino)ferrocene]palladium (II) was obtained from Stream. All reagents were purchased with reagent grade and used without further purification. Solvents were dried and used freshly distilled, unless otherwise specifically indicated. Thin layer chromatography (TLC) was performed on 0.25 mmsilic gel pre-coated plastic sheets (40/80 mm) (Polygram_ SIL G/UV254, Macherey & Nagel, Düren, Germany) using benzene/methanol (9/1) as eluent. The IR spectra were recorded on a FTIR Bomem-Michelson 102 spectrometer in the 4000–200 cm^{-1} region using CsI pellets. Conductivity values were obtained using 1.0 mmol·L^{-1} solutions of complexes in CH_2Cl_2, using a Meter Lab CDM2300 instrument. The molar conductance measurements (Λ_m) were carried out in dichloromethane at 25 °C, using concentrations of 1.0×10^{-3} mol·L^{-1} for the complexes. ^1H,$^{31}P\{^1H\}$ and ^{13}C NMR spectra were recorded on a Bruker DRX 400 MHz, internally referenced to TMS for hydrogen chemical shift (δ). The ^{31}P chemical shifts are reported in relation to H_3PO_4, 85%. $CDCl_3$ was used as solvent, unless mentioned. Partial elemental analyses were carried out on the Department of Chemistry of the Federal University of São Carlos, in an instrument of CHNS staff EA 1108 of the FISONS.

2.2. Synthesis of N,N-dialkyl-N′-(acyl/aroyl)thioureas

The *N*,*N*-disubstituted-*N*′-acylthioureas HL(1–8) used in this work were synthesized by the procedure previously reported in the literature [12]. A solution of an appropriate acyl chloride (30 mmol) in acetone (50 mL) was added dropwise to a suspension of KSCN (0.01 mol) in acetone (30 mL). The mixture was stirred until a precipitate appeared (ammonium chloride), indicating the formation of the respective organic isothiocyanate. The corresponding amine (40 mmol), dissolved in acetone was added slowly and with constant stirring to the resulting solution. The solution was cooled in an ice-water bath and the stirring was continued at room temperature during 2–9 h, until the reaction was completed (the reaction progress was monitored by TLC). The reaction mixture was then poured into 600 mL of cold water. The solid *N*,*N*-disubstituted-*N*′-(acyl/aroyl)thioureas were collected by filtration and finally purified by recrystallization from ethanol. The compounds were obtained as crystalline solids, in good yields. The identity of the products was confirmed by comparing their ^1H and ^{13}C NMR data with those reported in the literature [12]. The structures of the *N*,*N*-disubstituted-*N*′-acyl thioureas used as ligands in this work are shown in Fig. 1.

2.3. Synthesis of the complexes

The complexes were prepared as yellow solid products by a similar method to that used for $[Pd(PPh_3)_2Cl_2]$ [9] from direct reactions with the precursor $[Pd(dppf)Cl_2]$, with the *N*,*N*-disubstituted-*N*′-acylthioureas, in methanol solutions. The complexes were separated from the reaction mixtures as yellow crystalline solids. Filtration and further washing with hot water and hot hexane were enough to afford pure and stable compounds, in about 80% yields. Thus, the general procedure for the synthesis of the complexes is described: A solution of $[Pd(dppf)Cl_2]$ (1.46 g; 2.00 mmol) in 5 mL of methanol, was added dropwise to a solution of corresponding *N*,*N*-dialkyl-*N*′-(acyl/aroyl)thiourea (2.00 mmol), dissolved in 30 mL of the same solvent, and 0.368 g (2.00 mmol) of KPF_6. The reaction was heated under magnetic stirring at about 80 °C, for 2 h. The reaction mixture was left in the refrigerator overnight. The yellow solids obtained were filtered off and washed, successively, with hot water and hot hexane (3×20 mL). The obtained compounds are stable in the air and in dimethylsuphoxide solutions, for at least 72 h, as showed $^{31}P\{^1H\}$ NMR experiments.

The ^1H, ^{13}C and $^{31}P\{^1H\}$ NMR, IR and the elemental analyses, melting point temperature and molar conductivity (Λ_m, 1.0×10^{-3} mol L^{-1} in CH_2Cl_2) for the complexes (**1**–**8**) are listed below and the other data used for the characterization of the complexes will be find in the text:

(**1**) $[Pd(dppf)(N,N\text{-dimethyl-}N'\text{-benzoylthioureato-}k^2O,S)]PF_6$: ^1H NMR, δ: 7.86–7.81 (m, 5H, Ph); 7.64–7.51 (m, 5H), 7.37–7.17 (m, 10H), 3.48 (3H, s, CH_3), and 3.18 (3H, s, CH_3). NMR ^{13}C, δ: 169.7 (C=S); 161.8 (C=O); 134.5, 134.4, 134.4, 134.2, 134.1, 132.7–127.7 (C-Ph), 29.7 (CH_3), 15.3 (CH_3), $^{31}P\{^1H\}$ NMR, δ, 41.12 (d); 28.06 (d); $^2J_{P\text{-}P}$ = 19.43 Hz; IR, cm^{-1}: ν(C=O) 1416, ν(C=S) 747; ν(C=N) 1502; Anal. (%): Found (Calc) for $C_{44}H_{39}F_6FeN_2OP_3PdS$: C, 52.26 (52.17); H, 3.90 (3.88); N, 2.82 (2.77); S, 3.21 (3.17). Λ_m = 48.6 Ω^{-1} cm^2 mol^{-1}.

(**2**) $[Pd(dppf)(N,N\text{-diethyl-}N'\text{-benzoylthioureato-}k^2O,S)]PF_6$: ^1H NMR, δ: 7.87–7.82 (m, 1H), 7.61–7.48 (m, 5H), 7.36–7.31 (m, 5H), 7.15–6.99 (m, 10H), 3.81 (d, J = 7.07 Hz, 2H, CH_2), 3.58 (d, J = 7.07 Hz, 2H, CH_2), 1.28 (t, J = 7.02, 7.02 Hz, 3H, CH_3), 1.31 (t, J = 7.02, 7.02 Hz, 3H, CH_3); NMR ^{13}C, δ: 170.0 (C=S); 169.6 (C=O); 135.7, 135.6, 134.6, 134.5, 134.2–127.5 (C-Ph), 47.3 (CH_2), 46.5 (CH_2), 13.1 (CH_3), 12.1 (CH_3); $^{31}P\{^1H\}$, δ: 41.27 (d); 27. 41 (d); $^2J_{P\text{-}P}$ = 21.86 Hz; IR, cm^{-1}: ν(C=O) 1414, ν(C=S) 750; ν(C=N) 1501; Anal. (%): Found (Calc) for $C_{46}H_{43}F_6FeN_2OP_3PdS$: C, 53.15 (53.07); H, 4.08 (4.16); N, 2.70 (2.69); S, 3.00 (3.08). MP: 270–272 °C, Λ_m = 44.6 Ω^{-1} cm^2 mol^{-1}.

(**3**) $[Pd(dppf)(N,N\text{-dibutyl-}N'\text{-benzoylthioureato-}k^2O,S)]PF_6$: ^1H NMR, δ: 8.04–7.99(m, 1H), 7.80–7.08 (m, 34H), 4.88 (d, J = 7.08 Hz, 2H, CH_2), 3.68 (4H, q, CH_2), 2.07–1.70 (2H, m, CH_2), 0.93 (3H, t, CH_3, J = 7.01 Hz). NMR ^{13}C, δ: 170.6 (C=S), 168.5 (C=O), 135.6, 135.3, 135.2, 133.6–128.8 (C-Ph), 53.6 (CH_2), 52.4 (CH_2), 20.9 (CH_2), 14.2 (CH_3); $^{31}P\{^1H\}$, δ: 41.18 (d); 27. 63 (d); $^2J_{P\text{-}P}$ = 20.26 Hz; IR, cm^{-1}: ν(C=O) 1495, ν(C=S) 747; ν(C=N) 1495; Anal. (%): Found (Calc) for $C_{50}H_{51}F_6FeN_2OP_3PdS$: C, 54.54 (54.74); H, 4.65 (4.68); N, 2.53 (2.55); S, 2.85 (2.92), MP: 230–232 °C, Λ_m = 47.6 Ω^{-1} cm^2 mol^{-1}.

(**4**) $[Pd(dppf)(N,N\text{-diphenyl-}N'\text{-benzoylthioureato-}k^2O,S)]PF_6$: ^1H NMR, δ: 7.86–7.82 (m, 1H), 7.14 (s, 1H), 6.73 (d, J = 1.60 Hz, 1H), 6.86–6.83 (m, 1H),NMR ^{13}C, δ: 174.6 (C=S); 172.9 (C=O); 144.0, 143.1, 134.4, 134.3, 134.2, 134.1–127.3 (C/Ph). $^{31}P\{^1H\}$, δ:

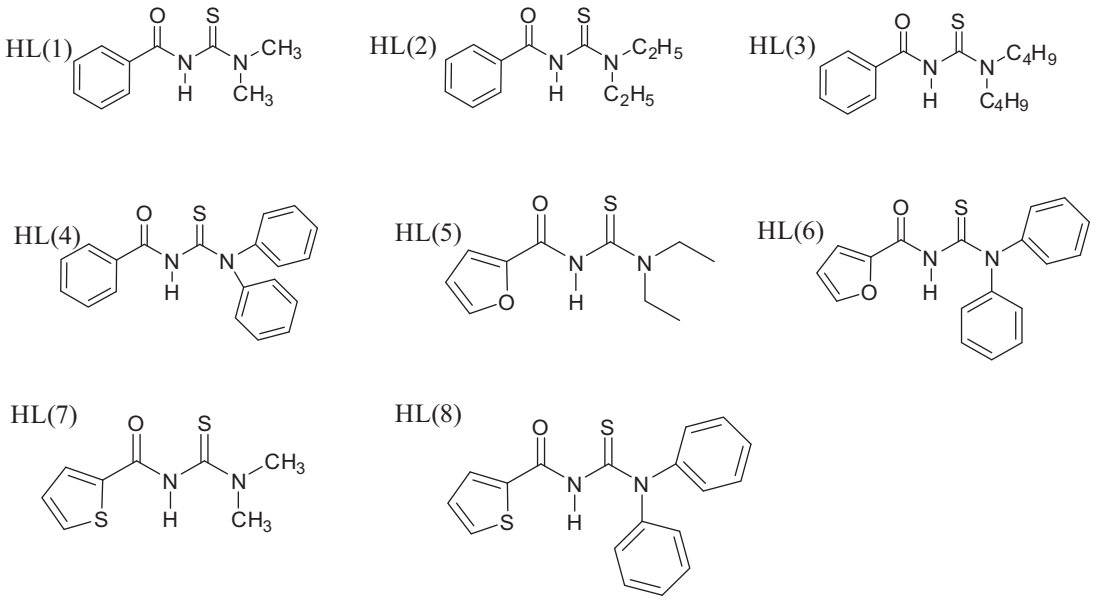

Fig.1. Structures of the *N*,*N*-disubstituted-*N*′-acyl thioureas used as ligands in this work.

41.25 (d), 27.58 (d) $^2J_{P\text{-}P}$ = 20.26; IR, cm^{-1}: *ν*(C=O) 1430, *ν*(C=S) 752; *ν*(C=N) 1494; Anal. (%): Found (Calc) for $C_{54}H_{43}F_6FeN_2OP_3PdS$: C, 56.98 (57.03); H, 3.90 (3.81); N, 2.37 (2.46); S, 2.78 (2.82). MP: 275–277 °C, Λ_m = 48.6 Ω^{-1} cm^2 mol^{-1}.

(**5**) [Pd(dppf)(*N*,*N*-diethyl-*N*′-furoylthioureato-k^{2}O,S)]PF_6: ^{1}H NMR, *δ*: 7.85–7.80 (m, 1H), 7.60–6.18 (3H, m, furoyl), 3.74 (2H, d, CH_2), 3.34 (2H, d, CH_2), 1.22 (3H, t, CH_3), 0.95 (3H, t, CH_3). NMR ^{13}C, *δ*: 165.7 (C=S), 159.8 (C=O), 145.9, 134.6, 134.5, 134.1–129.4 (C-Ph), 128.8–112.0 (C-Ph and furan ring), 47.2 (CH_2), 46.5 (CH_2), 13.1 (CH_3) 11.9 (CH_3). ^{31}P{^{1}H}, *δ*: 41.45 (d), 27.32 d); $^2J_{P\text{-}P}$ = 19.43, IR, cm^{-1}: *ν*(C=O) 1474., *ν*(C=S) 747; *ν*(C=N) 1504; Anal. (%): Found (Calc): Anal. (%): Found (Calc) for $C_{44}H_{41}F_6FeN_2O_2P_3PdS$: C, 51.15 (51.26); H, 3.97 (4.00); N, 2.68 (2.72); S, 3.09 (3.11). MP: 242–244 °C, Λ_m = 48.6 Ω^{-1} cm^2 mol^{-1}.

(**6**) [Pd(dppf)(*N*,*N*-diphenyl-*N*′-furoylthioureato-k^{2}O,S)]PF_6: ^{1}H NMR, *δ*: 7.91–7.80 (m, 1H), 7.63–7.43 (m, 1H), 7.20–6.99 (m, 1H), 6.53–6.16 (m, 1H), 4.98 (s, 2H, CH_2), 4.77 (s, 2H, CH_2). NMR ^{13}C, *δ*: 167.7 (C=S); 162.0 (C=O); 149.5, 146.8, 146.1, 145.7, 145.2–112.3 (C-Ph), 53.5 (CH_2), 52.8 (CH_2).^{31}P {^{1}H}, *δ*: 41, 30 (d), 27,54 (d), $^2J_{P\text{-}P}$ = 19.43; IR, cm^{-1}: *ν*(C=O) 1486, *ν*(C=S) 741; *ν*(C=N) 1573; Anal. (%): Found (Calc) for $C_{52}H_{41}F_6FeN_2O_2P_3PdS$: C, 55.39 (55.41); H, 3.61 (3.66); N, 2.45 (2.49); S, 2.80 (2.84). MP: 264–266 °C., Λ_m = 52.6 Ω^{-1} cm^2 mol^{-1}.

(**7**) [Pd(dppf)(*N*,*N*-dimethyl-N′- thiophenylthioureato-k^{2}O,S)] PF_6: ^{1}H NMR, *δ*: 8.02 (1H, dd, *J1* = 7.2 Hz, *J2* = 8.1 Hz, thiophene CH), 7.87 (1H, dd, *J1* = 7.59 Hz, *J2* = 8.2 Hz, thiophene CH), 6.70 (1H, dd, *J1* = 6.7 Hz, *J2* = 8.6 Hz, thiophene CH), 7.59–7.27 (C-Ph) 0.97 (6H, t, CH_3, *J* = 7.1 Hz), NMR ^{13}C, *δ*: 166.7 (C=S); 164.1 (C=O); 141.2, 134.6, 134.5, 134.5, 134.4, 132.4, 132.3, 132.2, 131.7, 128.9–125.6 (C-Ph); 21.8 ($2CH_3$). ^{31}P{^{1}H}, *δ*: 41.58 (d), 27.97 (d), $^2J_{P\text{-}P}$ = 19.47; IR, cm^{-1}: *ν*(C=O) 1418, *ν*(C=S) 745; *ν* (C=N) 1494; : Anal. (%): Found (Calc) for $C_{42}H_{37}F_6FeN_2OP_3PdS_2$: C, 49.35 (49.50); H, 3.60 (3.66); N, 2.71 (2.75); S, 6.20 (6.29). MP: 245–247 °C., Λ_M = 50.6 Ω^{-1} cm^2 mol^{-1}.

(**8**) [Pd(dppf)(*N*,*N*-diphenyl-N′-thiophenylthioureato-k^{2}O,S)] PF_6: ^{1}H NMR, *δ*: 8.02 (1H, dd, *J1* = 7.2 Hz, *J2* = 8.1 Hz, thiophene CH), 7.90 (1H, dd, *J1* = 7.5 Hz, *J2* = 8.2 Hz, thiophene CH), 7.89 (1H, dd, *J1* = 6.7 Hz, *J2* = 8.3 Hz, thiophene CH), 7.82-7.13 (m, 10H, arom-H). NMR ^{13}C, *δ*: 173.7 (C=S); 166.2 (C=O); 144.1, 143.2, 140.8, 140.7, 134.7, 134.2, 134.1, 134.0, 133.9, 132.3, 128.5–127.8 (C-Ph); ^{31}P{^{1}H}, *δ*: 41.62 (d); 27. 63 (d); $^2J_{P\text{-}P}$ = 19.43 Hz; IR, cm^{-1}: *ν*(C=O) 1420, *ν*(C=S) 743; *ν*(C=N) 1479; Anal. (%) Found (Calc) for $C_{52}H_{41}F_6FeN_2OP_3PdS_2$: C, 54.45 (54.63); H, 3.49 (3.61); N, 2.41 (2.45); S, 5.54 (5.61). MP: 256–258 °C., Λ_M = 49.6 Ω^{-1} cm^2 mol^{-1}.

2.4. Crystal structure determination

Single crystals suitable for X-ray diffraction were obtained by slow evaporation of $CHCl_3$:n-hexane (3:1) solutions of the complexes **2**, **3**, **5**, **6** and **8**. Diffraction data were collected on an Enraf–Nonius Kappa-CCD diffractometer with graphite-monochromated Mo Ka radiation (*λ* = 0.71073 Å). The final unit cell parameters were based on all reflections. Data collections were performed using the COLLECT program [13]; integration and scaling of the reflections were performed with the HKL Denzo–Scalepack system of programs [14]. Absorption corrections were carried out using the Gaussian method [15]. The structures were solved by direct methods with SHELXS-97 [16]. The models were refined by full-matrix least-squares on F^2 by means of SHELXL-97 [17]. The projection views of the structures were prepared using ORTEP-3 for Windows [18]. Hydrogen atoms were stereochemically positioned and refined with the riding model. Data collections and experimental details are summarized in Table 1. Relevant interatomic bond lengths and angles are listed in Table 2. Also included are the CCDC deposit numbers for Supplementary crystallographic data.

2.5. Antimycobacterial activity assay

Antimycobacterial activities of each tested compound and of the standard drug ethambutol were determined in triplicate, in sterile 96-wel flat bottom microplates. The tested compound concentrations ranged from 0.087 to 25 μg/mL, and the ethambutol from 0.015 to 1.0 μg/mL. The microplate Alamar Blue assay [19] was used to measure the minimal inhibitory concentration (MIC) for the tested compounds (minimum concentration necessary to inhibit 90 % growth of *M. tuberculosis* H_{37}Rv ATCC 27294). The development of a pink color in the wells was taken as indicating bacterial growth and the maintenance of a blue color as the contrary. The fluorescence of the dye was measured in a SPECTRAfluor Plus microplate reader (Tecan*) in bottom reading mode with excitation at 530 nm and emission at 590 nm.

Table 1
Crystal data and refinement parameters for **2**, **3**, **5**, **6**, and **8** complexes.

Compound	**2**	**3**	**5**	**6**	**8**
Empirical formula	$C_{46}H_{43}F_6FeN_2OP_3PdS.\ CH_2Cl_2$	$C_{50}H_{51}F_6FeN_2OP_3\ PdS$	$C_{44}H_{41}F_6FeN_2O_2P_3PdS$	$C_{52}H_{41}F_6FeN_2O_2P_3PdS$	$C_{52}H_{41}F_6FeN_2O\ P_3PdS_2$
Formula weight	1125.97	1097.15	1031.01	1127.09	1143.15
Crystal system	monoclinic	monoclinic	monoclinic	triclinic	triclinic
Space group	$P2_1/c$	Pc	$P2_1/a$	$P\bar{1}$	$P\bar{1}$
T (K)	293	296		296	296
a (Å)	10.5650(2)	10.6147(5)	10.8430(2)	12.5827(3)	12.5960(3)
b (Å)	27.6270(8)	14.557(1)	28.8291(5)	13.8101(4)	13.8000(4)
c (Å)	16.8200(4)	16.325(1)	14.1096(2)	14.9739(4)	15.0780(4)
V (Å^3)	4861.2(2)	2506.2(3)	4406.77(13)	2453.78(12)	2479.3(1)
Z	4	2	4	2	2
D_{calc} (mg/m^3)	1.538	1.454	1.554	1.525	1.531
Absorption coefficient (mm^{-1})	0.981	0.846	0.958	0.868	0.899
$F(000)$	2280	1120	2088	1140	1156
θ range for data collection (°)	2.555–25.999	2.875–25.997	2.565–25.997	2.972–25.999	2.84–26.00
Index ranges	$-11 \le h \le 13$	$-12 \le h \le 13$	$-12 \le h \le 13$	$-15 \le h \le 15$	$-15 \le h \le 15$
	$-32 \le k \le 34$	$-17 \le k \le 17$	$-35 \le k \le 35$	$-17 \le k \le 16$	$-17 \le k \le 17$
	$-20 \le l \le 12$	$-20 \le l \le 16$	$-16 \le l \le 17$	$-18 \le l \le 18$	$-18 \le l \le 18$
Reflections collected	25156	12255	38378	25632	28331
Independent reflections (R_{int})	9351 [R_{int} = 0.0386]	7966 [R_{int} = 0.0592]	8639 [R_{int} = 0.0926]	9547 [R_{int} = 0.0481]	9719 [R_{int} = 0.0387]
Goodness-of-fit on F^2	1.024	1.044	1.026	1.019	1.070
Final R índices	R_1 = 0.0518	R_1 = 0.0603	R_1 = 0.0509	R_1 = 0.0479	R_1 = 0.0461
[I N 2σ (I)]	wR_2 = 0.1345	wR_2 = 0.1537	wR_2 = 0.1275	wR_2 = 0.1247	wR_2 = 0.1314
Largest diff. peak and hole (eÅ)$^{-3}$	0.848 and −0.631	0.779 and −0.487	0.888 and −0.810	0.623 and −0.794	1.160 and −0.794
CCDC deposit number	1502550	1502551	1502552	1502553	1502554

Table 2
Selected bond lengths (Å) and angles (°) for **2**, **3**, **5**, **6** and **8** complexes.

	2	**3**	**5**	**6**	**8**
Bond lengths (Å)					
Pd–O	2.046(3)	2.067(7)	2.032(3)	2.049(2)	2.053(2)
Pd–P(1)	2.261(1)	2.266(2)	2.255(1)	2.2578(9)	2.2620(8)
Pd–P(2)	2.356(1)	2.359(2)	2.35(1)	2.3478(9)	2.3527(8)
Pd–S	2.290(1)	2.295(2)	2.300(1)	2.2979(9)	2.2991(9)
S–C1	1.740(4)	1.73(1)	1.748(5)	1.721(4)	1.731(4)
O–C2	1.274(5)	1.26(1)	1.259(5)	1.267(4)	1.270(4)
C1–N1	1.335(6)	1.37(1)	1.333(6)	1.334(5)	1.329(5)
C2–N1	1.297(6)	1.29(1)	1.309(6)	1.317(5)	1.322(4)
Angles (°)					
O–Pd–S	91.88(9)	92.2(2)	90.9(1)	91.94(7)	92.16(7)
O–Pd–P(1)	178.8(1)	178.8(2)	176.0(1)	179.41(8)	178.67(9)
O–Pd–P(2)	84.53(9)	84.6(2)	84.1(1)	83.25(7)	83.86(7)
P(2)–Pd–S	175.94(4)	176.8(1)	174.41(4)	174.64(3)	174.29(3)
P(1)–Pd–S	88.43(4)	88.24(9)	90.42(4)	88.14(3)	87.58(3)
P(2)–Pd–P(1)	95.12(4)	94.99(8)	94.74(4)	96.70(3)	96.49(3)

2.6. Antiparasitic activity

Y strain trypomastigotes of *T. cruzi* collected from the LLC-MK2 cell supernatant were dispensed into 96-well plates at a cell density of 2.0×10^6 cells/mL in 200 μL of RPMI medium. Compounds were tested at eight concentrations from (10–0.01 μM), in triplicate. The plate was incubated for 24 h at 37 °C and 5% CO_2. Aliquots from each well were collected and the number of viable parasites, based on parasite viability, was assessed in a Neubauer chamber and compared to untreated parasite culture. This experiment was performed three times. Inhibitory concentration for 50 % (IC_{50}) was calculated using data-points gathered from three independent experiments. Benznidazole was used as a positive control.

2.7. Cytotoxicity in murine cells

J774 cells (murine macrophages cell line, established from a tumor that arose in female BALB/c mouse were placed on 96-well plates at a cell density of 5×10^4 cells/Ml in 200 μL of RPMI-1640 medium (no phenol red) and supplemented with 10% FBS and 50 μg/mL of gentamycin and incubated for 24 h at 37 °C and 5% CO_2. Compounds were added in a series of eight concentrations, in triplicate, and incubated for 72 h. Then, 20 μL/well of AlamarBlue (Invitrogen, Carlsbad, USA) was added to all wells and incubated during 6 h. Colorimetric readings were performed at 570 and 600 nm. Cytotoxic concentration for 50% (CC_{50}) was calculated using data-points gathered from three independent experiments. Gentian violet was used as a positive control.

2.8. Propidium iodide (PI) and annexin V staining

T. cruzi trypomastigotes from Y strain (1×10^7) were incubated for 24 h at 37 °C in the absence or presence of **1** (0.61 or 1.22 μM) or **4** (1.91 or 3.82 μM). After incubation, the parasites were labeled for PI and FITC-annexin V using the annexin V-FITC apoptosis detection kit (Sigma–Aldrich), according to the manufacturer's instructions. Acquisition and analyses was performed using a FACS Calibur flow cytometer (Becton Dickinson, San Diego, CA), with FlowJo software (Tree Star, Ashland, OR). A total of 10.000 events were acquired in the region previously established as that corresponding to trypomastigotes.

3. Results and discussion

The ligands were prepared following the procedures previously reported in the literature [12] and were obtained in yields ranging from 79% to 91%. The complexes of the type [Pd(dppf)(L)] were obtained by the reactions between [Pd(dppf)Cl_2] and the ligands (see Scheme 1). The synthesized complexes were yellowish crystals and their elemental analyses, melting point temperatures, and molar conductivities are listed in the experimental section. Complexes **2**, **3**, **5**, **6** and **8** were also characterized by single crystal X-ray diffraction.

The IR spectra of the complexes were compared with those of the free ligands. The N–H stretching vibrations which exist in the ligands disappear. A broad peak ascribed to the C–N bond appears around 1580–1600 cm^{-1}, indicating deprotonation of the acylthioureido group of the ligands during the complexes formation and therefore their coordination through the oxygen and sulfur atoms [20–22]. The bands observed around 471–490 cm^{-1} were assigned to M–O [23,24]. Assignment of the Pd-S stretching vibration bands at about 360 cm^{-1} are in accordance to the reported literature [25,26]. The bands in the 551–556 cm^{-1} range are assigned to M–N (imino nitrogen) [20]. Strong bands in the region of about 1500 cm^{-1}, are shown by the IR spectra of the complexes which may reasonably be assigned to the coordinated C–O groups. The absorption bands at 815–878 cm^{-1} in the spectra of free *N*,*N*-disubstituted-*N*′-acylthioureas, attributed to the ν(C–S) stretching vibrations, shift to the 837–845 cm^{-1} range in the complexes spectra, corresponding to the weakening of the C–S double bond character [21].

In the ^{1}H NMR spectra ($CDCl_3$) of the ligands HL(**1**–**8**), the NH proton appears at 8.79–8.45 ppm as broad singlets. This signal is absent in the ^{1}H NMR spectra of the corresponding palladium complexes, in the same solvent, as a consequence of the deprotonation of the nitrogen atom. Similarly, the IR spectra of the ligands HL(**1**–**8**) show NH stretching vibrations in the range 3150–3260 cm^{-1}, but these signals are absent in the spectra of the corresponding metal complexes. In the ^{13}C NMR spectra, the carbon atom of the thiocarbonyl group appears at δ = 165.67–173.67 in the metal complexes, as mentioned in the experimental section.

The ^{31}P{^{1}H} NMR spectra of the precursor [Pd(dppf)Cl_2], in CH_2Cl_2 solution, shows a singlet peak for phosphorus atoms at δ = 35.12. For all complexes two doublets arise, at about δ = 41.34 and 27.64, indicating the presence of two magnetically different phosphorus atoms coordinated to the palladium(II) ion. Also in the region of δ = −138–158 a multiple signal of the PF_6^-, functioning as outer-sphere anions for the complexes is observed, in accordance to the molar conductivity measurements for these complexes (see experimental section). These data are consistent with those obtained for some thiosemicarbazones and *N*,*N*-disubstituted-*N*′-acyl thioureas complexes [10,21,27].

The molecular structures of **2**, [Pd(dppf)(*N*,*N*-diethyl-*N*′-benzoylthioureato-k^{2}O,S)]PF_6, **3**, [Pd(dppf)(*N*,*N*-dibuthyl-*N*′-benzoylthioureato-k^{2}O,S)]PF_6, **5**, [Pd(dppf)(*N*,*N*-diethyl-*N*′-furoylthioureato-k^{2}O,S)]PF_6, **6**, [Pd(dppf)(*N*,*N*-diphenyl-*N*′-furoylthioureato-k^{2}O,S)]PF_6, and **8**, [Pd(dppf)(*N*,*N*-diphenyl-N′-thiophenylthioureato-k^{2}O,S)]PF_6, are shown in Fig. 2, and selected bond lengths and angles (°) for these structures are listed in Table 2.

In all complexes the Pd(II) ion is nearly planar, in a fourfold environment. The thione C–S bond in the coordinated anionic ligands becomes formally a single bond making it longer (average = 1.734 Å) than the C=S bond of the neutral moieties [27,28] (Fig. 2, Table 2). Thus the metal is coordinated to the negatively charged organic molecules, which act as bidentate ligands, through oxygen (average distance Pd–O = 2.0494 Å) and sulfur (average distance Pd–S = 2.2964 Å) atoms. The Pd–S average distance is close to the ones found for other palladium(II) thiosemicarbazones complexes [21]. The remaining binding sites are occupied by biphosphines (dppf) (average distance Pd–P1 = 2.2604 Å and Pd–P2 = 2.3531 Å). The distances for the C–S and C–O bonds in the chelate rings, listed in Table 2, are the characteristic of single and double bond lengths, respectively [9,21,27]. The N1–C1 and N2–N1 bond distances (average 1.3402 Å and 1.307 Å, respectively) present typical bond lengths of double bond character, suggesting an electron delocalization in the acyl thiourea moiety [21–27]. The C–O bond distances are slightly sensitive to the coordination of the ligand to the metal. In previously work it was reported, on the bis-triphenylphosphine-N,N-dietyl-N′-furoylthioureato-k2O,S, that the C–O distance for the free ligand is 1.226(3) Å (average for two independent molecules per asymmetric unit), and 1.266(9) Å (average), after its coordination to the metal [28].

After structural characterization, the metal-free *N*,*N*-disubstituted-*N*′-acylthioureas and metal complexes were investigated for their *in vitro* antimycobacterial activity against *M. tuberculosis* H37Rv strain and antiparasitic activity against Y strain *T. cruzi* trypomastigotes. The results are displayed in Table 3.

None the metal-free ligands presented antimycobacterial activity in concentration below 70 μM, while the palladium complexes presented activity in the same micromolar range as observed under Ethambutol treatment. Therefore, the presence of palladium is essential to improve the antimycobacterial activity of the free ligands. Regarding structure–activity relationships, the main difference between most and less active Pd(II) complexes is the presence of a linear and alkyl side chain attached at R2 in the ligand structure. This may be the reason for the decreased the antimycobacterial activity of complexes **4**, **6** and **8** in comparison to **1**, **2**, **3**, **5** and **7**.

Next, the antiparasitic activity was analyzed and the results were compared to the reference drug benznidazole, which displayed an IC_{50} value of 10.61 ± 0.87 μM. None the metal-free ligands displayed antiparasitic activity, while the Pd(II) complexes

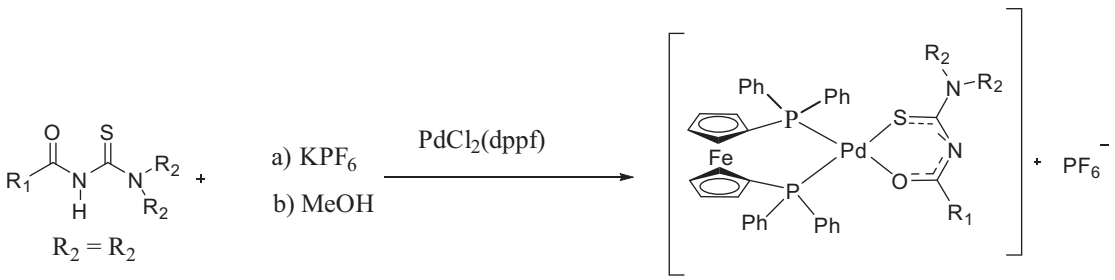

Scheme 1. Route for the syntheses of [Pd(dppf)(*N*,*N*-disubstituted-*N*′-acylthiourea)]PF_6 complexes.

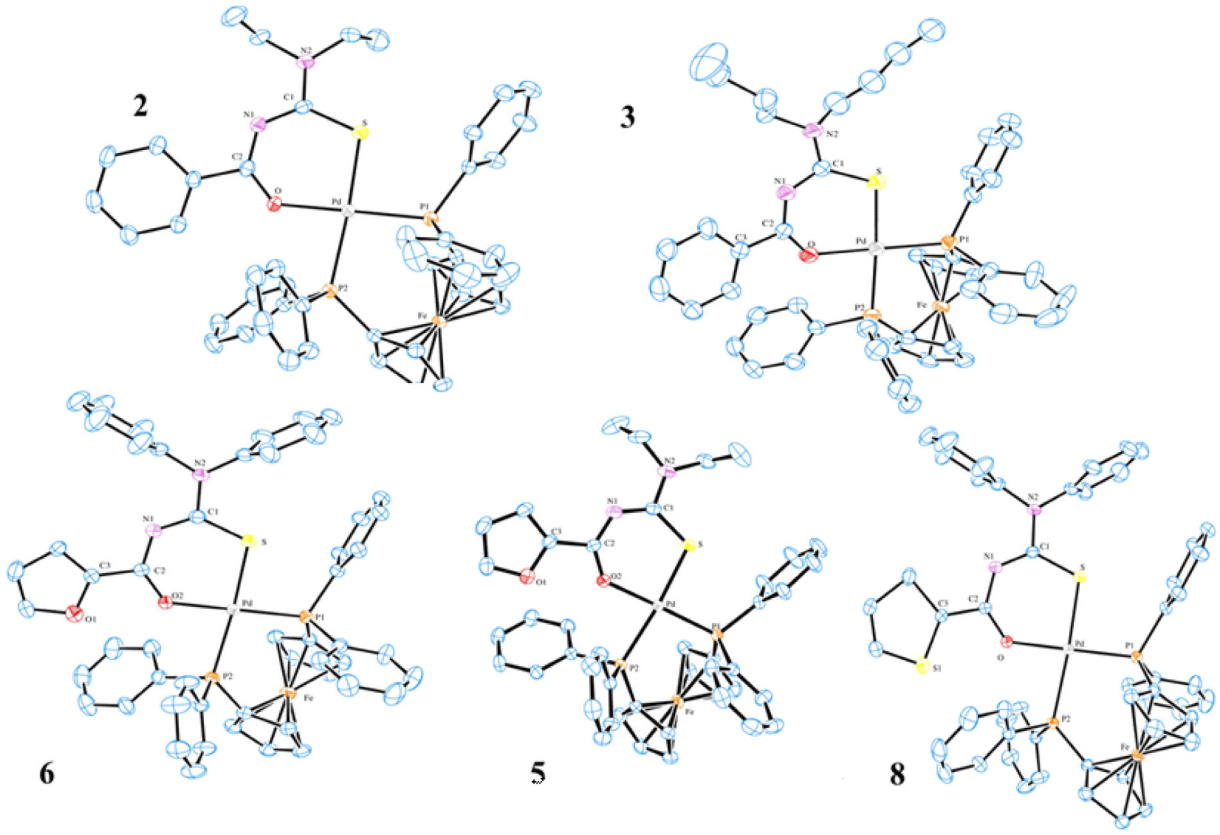

Fig. 2. ORTEP view of complexes **2**, **3**, **5**, **6** and **8** showing 50% probability ellipsoids. The $(PF_6)^-$ anion and some labels of the ligands are omitted for clarity. For complex **2** there is a CH_2Cl_2 solvated molecule, which was also omitted.

Table 3
Antimycobacterial, antiparasitic and cytotoxicity activity of ligands and complexes **1**–**8**.

Compound	*M. tuberculosis* H_{37}Rv MIC (μM)[a]	*T. cruzi* IC_{50} ± S.E.M. (μM)[b]	Cytotoxicity CC_{50} ± S.D. (μM)[c]	SI [d]
HL (**1**)	>119.6	>10	>30	–
HL (**2**)	>100.3	>10	>30	–
HL (**3**)	>85.6	>10	>30	–
HL (**4**)	>75.3	>10	>30	–
HL (**5**)	>110.6	>10	>30	–
HL (**6**)	>75.3	>10	>30	–
HL (**7**)	>116.8	>10	>30	–
HL (**8**)	>73.9	>10	>30	–
1	2.58 ± 0.38	0.61 ± 0.27	2.63 ± 1.25	4.3
2	2.82 ± 0.04	0.53 ± 0.21	1.53 ± 0.50	2.9
3	5.24 ± 0.33	1.47 ± 0.47	4.14 ± 1.35	2.8
4	17.32 ± 0.20	1.91 ± 0.50	8.83 ± 1.60	4.6
5	2.98 ± 0.02	0.76 ± 0.20	2.27 ± 0.64	3.0
6	6.36 ± 0.16	1.91 ± 0.70	3.86 ± 0.35	2.0
7	2.88 ± 0.07	0.55 ± 0.07	1.85 ± 0.48	3.3
8	9.71 ± 1.12	1.59 ± 0.04	5.83 ± 0.72	3.7
Ethambutol	5.62	–	–	–
Benznidazole	–	10.61 ± 0.87	>30	>2.8
Gentian Violet	–	–	0.82 ± 0.12	–

[a] Determined after 7 days incubation time with the drugs.
[b] Determined in trypomastigotes after 24 h incubation.
[c] Determined in J774 macrophages after 72 h incubation.
[d] SI = selectivity index for antiparasitic activity, determined as CC_{50}(cytotoxicity)/IC_{50} (trypomastigotes).

exhibit antiparasitic activity. In general, the metal complexes were more potent antiparasitic agents than benznidazole, however, they presented lower selectivity indexes than benznidazole. After observing that palladium complexes exhibit antiparasitic activity, it was investigated how the complexes can cause parasite cell death. To this end, trypomastigotes were treated with the IC_{50} or IC_{99} concentration of complexes **1** and **4** for 24 h and then stained with PI/annexin (Fig. 3).

In comparison to untreated parasites, treatment with complex **1** at IC_{50} concentration increased from 2.2 to 11.5 % cells positively stained for annexin. When the complex **1** was added at IC_{99} concentration, the % of annexin-stained cells changed from 11.5 to

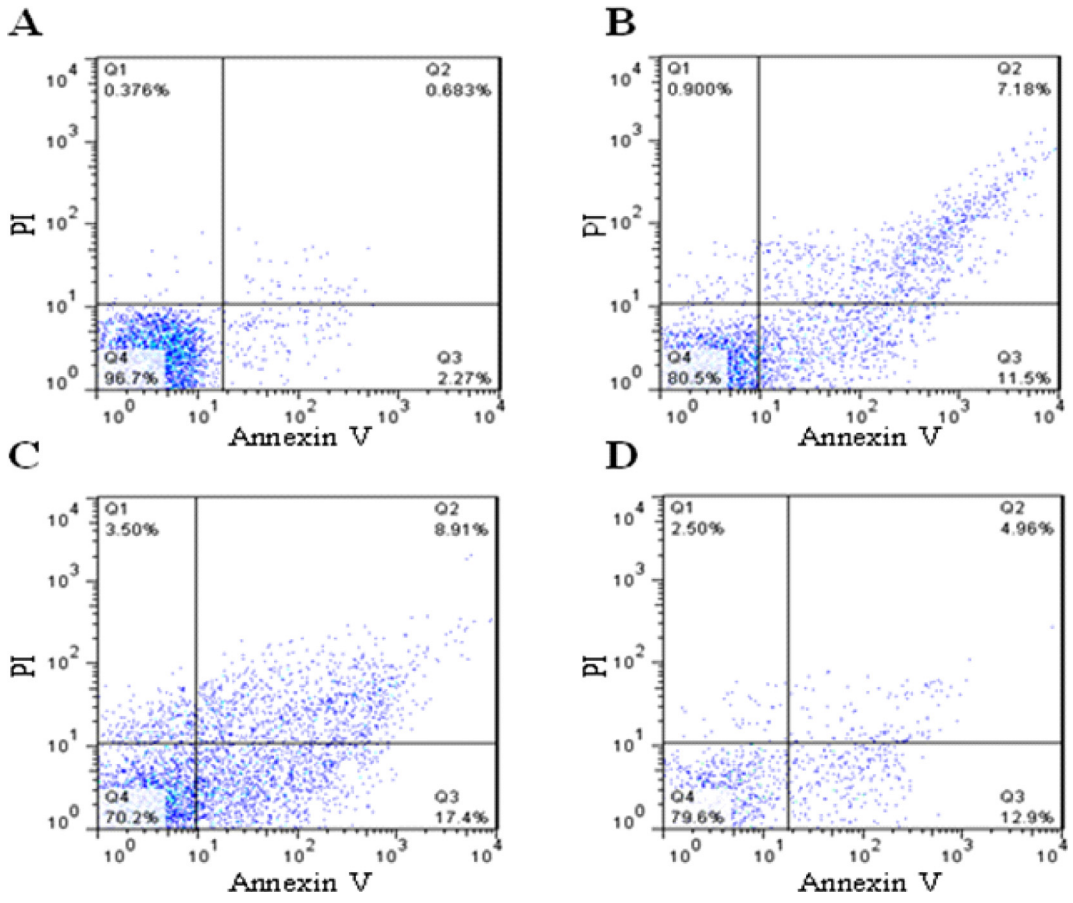

Fig. 3. Flow cytometry analysis of trypomastigotes (Ystrain) treated with **1** or **4** for 24 h and stained with PI and annexin V. (A) Representative untreated trypomastigotes; (B) trypomastigotes treated with **1** (0.61 μmol L^{-1}); (C) trypomastigotes treated with **1** (1.22 μM); (D) trypomastigotes treated with **4** (1.91 μM). Three independent experiments were performed, here on representative experiment is shown.

17.4, indicating that complex acts in a concentration-dependent manner. It was also observed that complex **1** treatment increased the double staining for PI/annexin. A similar cell death was also observed when complex **4** was evaluated. The single and double staining observed here for these complexes are indicative that parasite cell death occurs through an apoptosis process. Antiparasitic properties of palladium complexes have been observed as causing apoptotic cell death [29], while other metal transition complexes usually cause a necrotic death [30].

4. Conclusions

A novel series of Pd(II)/*N*,*N*-disubstituted-*N*′-acyl thioureas is here reported. The IR and NMR data suggest the coordination of the ligands to the metal center occurs bidentately, through the oxygen and sulfur atoms, which was confirmed by X-ray crystallographic characterization for complexes **2**, **3**, **5**, **6** and **8**. *In vitro* screening of complexes against *M. tuberculosis* and *T. cruzi* revealed that metal-free ligands were inactive, while complexes were activity. Structure–activity relationship indicated that their activity are dependent of the R2 group present in the amine nitrogen, while the nature of R1, attached in the acyl group, was less important for activity. The findings observed here reinforce that palladium are valuable antiparasitic agents.

Acknowledgments

This work was supported by the Brazilian sponsors: CAPES (Project Oficio/CSS/CGCI/ 23038009487/2011-25/DRI/CAPES, AUX CAPES-MES-Cuba, 339/2011), CNPq, FAPESP (Processo 2014/13691-4) and FAPESB.

Appendix A. Supplementary data

CCDC 1502550, 1502551, 1502552, 1502553 and 1502554 contains the supplementary crystallographic data for complexes **2**, **3**, **5**, **6** and **8**. These data can be obtained free of charge via http://dx.doi.org/10.1016/j.poly.2017.05.003, or from the Cambridge Crystallographic Data Centre, 12 Union Road, Cambridge CB2 1EZ, UK; fax: (+44) 1223-336-033; or e-mail: deposit@ccdc.cam.ac.uk.

References

[1] Global Alliance for TB Drug Development.www.tballiance.org [accessed 01.06.2016].
[2] T.D. Primm, S.G. Franzblau, Curr. Bioact. Compd. 6 (2007) 201.
[3] C.J. Schofield, C.J. Jannin, J.R. Salvatella, Trends Parasitol. 12 (2006) 583.
[4] S. Antinori, R. Grande, R. Bianco, L. Traversi, C. Cogliati, D. Torzillo, E. Repetto, M. Corbellino, L. Milazzo, M. Galli, L. Galimberti, Clin. Infect. Dis. 60 (2015) 1873.
[5] J.A. Urbina, Acta Trop. 115 (2010) 55.
[6] H. Pervze, H.P. Iqbal, M.Y. Tahir, F.H. Nasim, M.I. Choudhary, K.M. Khan, J. Enzym. Inhib. Med. Chem. 23 (2008) 848.
[7] D.C. Greenbaum, Z. Mackey, E. Hansell, P. Doyle, J. Gut, C.R. Caffrey, J. Lehrman, P.J. Rosenthal, J.H. Mckerrow, K. Chibale, J. Med. Chem. 47 (2004) 3212.
[8] G.M. Dobrikov, V. Valcheva, Y. Nikolova, I. Ugrinova, E. Pasheva, V. Dimitrov, Eur. J. Med. Chem. 63 (2013) 468.
[9] A.M. Plutín, R. Mocelo, A. Alvarez, R. Ramos, E.E. Castellano, Marcia R. Cominetti, A.E. Graminha, A.G. Ferreira, A.A. Batista, J. Inorg. Biochem. 134 (2014) 76.
[10] R.S. Correa, K.M. de Oliveira, F.G. Delolo, A. Alvarez, R. Mocelo, A.M. Plutin, M.R. Cominetti, E.E. Castellano, A.A. Batista, J. Inorg. Biochem. 150 (2015) 63.

[11] H. Arslan, N. Duran, G. Borekci, C.K. Ozer, C. Akbay, Molecules 14 (2009) 519.
[12] A. Plutin, H. Márquez, M. Morales, M. Sosa, L. Morán, Y. Rodríguez, M. Suárez, C. Seoane, N. Martín, Tetrahedron 56 (2000) 1533.
[13] Enraf-Nonius, Collect, Nonius BV, Delft, The Netherlands, 1997–2000.
[14] Z. Otwinowski, W. Minor, Processing of X-ray diffraction data collected in oscillation mode, Macromol. Crystallogr. A 276 (1997).
[15] R.H. Blessing, Acta Crystallogr. A 51 (1995) 33.
[16] G.M. Sheldrick, ShelXS-97 Program for Crystal Structure Resolution, University of Göttingen, Göttingen, Germany, 1997.
[17] G.M. Sheldrick, ShelXL-97, University of Göttingen, Göttingen, Germany, Program for Crystal Structures Analysis, 1997.
[18] L.J. Farrugia, J. Appl. Crystallogr. 30 (1997) 565.
[19] L.A. Collins, S.G. Franzblan, Antimicrob. Agents Chemother. 41 (1997) 1004.
[20] A.E. Graminha, C. Rodrigues, A.A. Batista, L.R. Teixeira, E.S. Fagundes, H. Beraldo, Spectrochim. Acta A 69 (2008) 1073.
[21] P. I.da S. Maia, A.E. Graminha, F.R. Pavan, C.Q.F. Leite, A.A. Batista, D.F. Back, E.S. Lang, J. Ellena, S. de S. Lemos, H.S. Salistre-de-Araujo, V.M. Deflon, J. Braz. Chem. Soc. 21 (2010) pp. 1177.
[22] A.P. Rebolledo, M. Vieites, D. Gambino, O.E. Piro, E.E. Castellano, C.L. Zani, E.M. Souza-Fagundes, L.R. Teixeira, A.A. Batista, H. Beraldo, J. Inorg. Biochem. 99 (2005) 698.
[23] K. Nakamoto, Infrared and Raman Spectra of Inorganic and Coordination Compounds, fourth ed., Wiley, New York, 1986.
[24] A. Pérez-Rebolledo, O.E. Piro, E.E. Castellano, L.R. Teixeira, A.A. Batista, H. Beraldo, J. Mol. Struct. 794 (2006) 18.
[25] B.H. Abdullah, Y.M. Salh, Orient. J. Chem. 26 (2010) 763.
[26] M.N. Patel, C.R. Patel, H.N. Joshi, P.A. Vekariya, Appl. Biochem. Biotechnol. 172 (2014) 1846.
[27] A.M. Plutin, A. Alvarez, R. Mocelo, R. Ramos, E.E. Castellano, M.M. da Silva, L. Colina-Vegas, Fernando R. Pavan, A.A. Batista, Inorg. Chem. Com. 63 (2016) 74.
[28] B. O'Reilly, A.M. Plutín, H. Pérez, O. Calderón, R. Ramos, R. Martínez, R.A. Toscano, J. Duque, H. Rodríguez-Solla, R. Martínez-Alvarez, M. Suárez, N. Martín, Polyhedron 36 (2010) 133.
[29] A.L. Matsuo, L.S. Silva, A.C. Torrecilhas, B.S. Pascoalino, T.C. Ramos, E.G. Rodrigues, S. Schenkman, A.C. Caires, L.R. Travassos, Antimicrob. Agents Chemother. 54 (2010) 3318.
[30] T. M. Bastos, M. I. Barbosa, M. M. da Silva, J. W. da C. Júnior, C. S. Meira, E. T. Guimaraes, J. Ellena, D. R. Moreira, A. A. Batista, M. B. Soares, Antimicrob Agents Chemother, 58 (2014) pp. 6044.